ELSEVIER

Carbohydrate Research 268 (1995) 267–277

CARBOHYDRATE RESEARCH

Subsite mapping of porcine pancreatic alpha-amylase I and II using 4-nitrophenyl-α-maltooligosaccharides

El Hassan Ajandouz, Guy J. Marchis-Mouren *

Laboratoire de Biochimie et Biologie de la Nutrition, URA-CNRS 1820, Université d'Aix-Marseille III, Faculté des Sciences, Avenue Escadrille Normandie-Niemen, F-13397 Marseille, France

Received 28 June 1993; accepted in revised form 8 October 1994

Abstract

The catalytic efficiency (k_{cat}/K_m) and the cleaved bond distribution for the nitrophenylated maltooligosaccharides, p-NPGlc$_n$ ($2 \leqslant n \leqslant 7$) hydrolysed by porcine pancreatic alpha-amylase isozymes I and II were determined. The subsite affinities (A_i) were calculated from the p-NPGlc$_n$ ($4 \leqslant n \leqslant 7$) hydrolysis data. Five subsites (-3 to 2) bind glucosidic residues with a positive affinity. No additional subsites could be detected both at the reducing end (3, 4, 5) and at the nonreducing end (-4, -5, -6). The energetic profiles of both isozymes are similar. The energetic profile of PPA differs from other alpha-amylases by having both a small number of subsites, and a catalytic subsite with a high positive affinity. Excellent agreement was found between observed catalytic efficiency values and those calculated from the subsite affinities.

Keywords: alpha-Amylase isozymes; Active centre; Subsite structure; Energetic profile; Porcine pancreatic alpha-amylase

1. Introduction

Alpha-amylases [α-(1 → 4)-glucan-4-glucanohydrolase EC 3.2.1.1] are endoglucanases, acting both as hydrolases and as transferases in condensation and/or transglycosylation reactions, depending on substrate concentration [1]. Alpha-amylases are widely distributed in animals, plants, bacteria and fungi. Their structure and function are well documented [2]. Porcine alpha-amylase isozymes (PPA I and PPA II) are secreted

* Corresponding author. Phone: (33) 91.28.81.10. Fax: (33) 91.28.84.40.

SSDI 0008-6215(94)00335-1

in about equal amounts in the pancreatic juice [3]. They differ in their isoelectric points, but their molecular weights and properties appear identical. X-ray diffraction studies on PPA I [4–6], two closely related fungal alpha-amylases [7,8] and barley malt amylase[9] as well as structure prediction of several other alpha-amylases [10,11], show that these enzymes belong to the family of $(\beta/\alpha)_8$-barrel enzymes [12]. The location of substrate analogues and inhibitors in the crystallized molecule has been found deep in a 3 nm cleft (the active site) by difference Fourier analysis [4,13,14].

From enzymological studies, the active site of PPA consists of an array of 5 consecutive binding subsites, each of which interacts with a single substrate glucosyl residue [1]. The catalytic subsite (see Fig. 3, arrow) is located between the 2nd (1) and the 3rd (-1) subsite from the reducing end.

Studies with amylose, maltooligosaccharides, and their nitrophenylated derivatives show that full amylase activity (PPA II) is obtained only when the five subsites are occupied [15]. The bond cleavage frequencies and respective kinetic parameters for short substrates ($2 \leqslant n \leqslant 4$) were used for calculation of glucosyl residue binding energies. The subsite energy profile thus obtained is characterized by a low affinity for D-glucose at the catalytic subsite.

In the present work, a series of nitrophenylated oligosaccharide substrates ($2 \leqslant n \leqslant 7$) was used. Catalytic efficiencies [16] and bond cleavage frequencies were determined at the lowest possible substrate concentration, in order to limit transglycosylation [1]. Binding energies were calculated using substrates with four glucosyl residues or more. The energetic profiles of PPA I and PPA II are compared.

2. Experimental

Materials. — Amylose (DP 410) was from Sigma, 4-nitrophenyl-α-D-maltooligosaccharides were from Boehringer, Mannheim. PPA I and PPA II were purified as previously described [17], except that phenylmethylsulfonyl fluoride (PMSF), 20 μM, was present at all stages of purification. The isozymes were concentrated by ultrafiltration through a PM 10 membrane (Amicon) to about 10 mg/mL, dialysed against 20 mM sodium phosphate (pH 6.9) containing 6 mM NaCl, 1 mM NaN_3 and 20 μM PMSF.

Methods. — Incubations, in the same buffer as above, were carried out at 30°C for 2, 5, 8, 12, 16, and 20 min (p-$NPGlc_2$), 20, 40, 60, 80, 100, and 120 s (p-$NPGlc_3$), 15, 30, 45, 60, 75, and 90 s for longer substrates.

Reactions were initiated by addition of enzyme (2.5 nM–34 μM) to the digests. Samples were taken at appropriate time intervals and the reaction was stopped by mixing with 1 vol of 1 M AcOH at 0°C and finally lyophilized. Digestion products (p_i) and remaining substrate (S) were separated by LC using a Merck Lichrospher-100-diol column (0.39 × 30 cm) in 80% MeCN–water (v/v) at room temperature and a flow rate of 0.5 mL min^{-1}. Eluates was monitored at 313 nm and nitrophenylated compounds quantified by using relevant standards. The cleavage frequency ($p_i/\Sigma p_i$) was expressed as mol fraction. Incubations using amylose as substrate (0.05%, w/v) were performed in the same buffer. The reaction velocity was followed by reductometry [18]. The concentration of the reducing products from amylose hydrolysis was expressed in maltose equivalents assuming that 1% amylose solution = 29.3 mM maltose [15].

Theoretical methods. — Depolymerase (E) can accommodate homopolymeric substrate (S_n) containing n (glucosyl) residues. Due to the subsite (i) organization of the active site, several complexes (ES_n) can be present depending on the subsites occupied. Each one is defined by its binding mode j, where j is the subsite number occupied by the p-nitrophenyl moiety present at the reducing end. Only complexes in which subsites -1 and 1 are occupied, are productive. Assuming rapid equilibrium between E and ES_n:

$$k_{cat}/K_m = k_{int}\sum K_{n,p}$$

$K_{n,p}$, the association constant for a productive ES_n complex in the binding mode j, is related to the molecular binding affinity $B_{n,j}$ which is the unitary part of standard affinity, $\Delta G_{n,j}$ [19]:

$$RT \ln K_{n,p} = -\Delta G_{n,j} = B_{n,j} + \text{constant}$$

Assuming subsite additivity:

$$B_{n,j} = \sum_i A_i$$

One can obtain A_i [16] either from:

$$B_{n,j} - B_{n-1,j}$$

or

$$B_{n,j} - B_{n-1,j-1}$$

Considering that k_{int}, the intrinsic rate constant of hydrolysis, is the same for each substrate:

$$\exp(A_i/RT) = (k_{cat}/K_m)_n \cdot \left(p_i / \sum_1^{n-1} p_i \right) / (k_{cat}/K_m)_{n-1} \cdot \left(p_{i-1} / \sum_1^{n-2} p_i \right)$$

The catalytic efficiency k_{cat}/K_m was determined at low substrate concentration from the $\ln(S_0/S)$ vs. t plot, where S_0 is the initial and S the substrate concentration at the time t [16]. Values of the slopes giving k_{cat}/K_m were calculated by linear regression. The product (p_i) liberated at various times of incubation allows to calculate the cleavage frequency ($p_i/\sum p_i$).

The number of subsites is given by those that bind glucosyl residues with significant affinity value.

3. Results

Characterization of porcine pancreatic alpha-amylase isozymes. — Analysis by isoelectric focusing gives a single band with pI 7.5 and 6.4 for PPA I and PPA II respectively (Fig. 1). The entire PPA I 496-aminoacid residue sequence [20,21] and a partial sequence [22] (243 residues) of PPA II have been determined. Comparison of the homologous sequences indicate some amino acid changes: Q41A, E76N, N87D, N184D, K243R, E352Q, and E404Q, which account for the difference in isoelectric points. Still

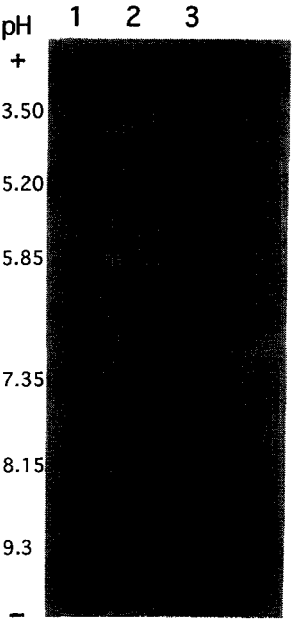

Fig. 1. Isoelectric focusing of the isozymes of porcine pancreatic alpha-amylases. Lane 1, pI standards; lane 2, PPA I; lane 3, PPA II.

no difference between the 3D structures of PPA I and PPA II at 2 Å resolution could be detected [23]. Also no functional differences have been reported.

Kinetic studies and product analysis: comparison of PPA I and PPA II. — As a first approach to determine subsite binding affinities, the method described by Thoma et al. [24] was applied to PPA I. Incubation were at 0.2 K_m to 5 K_m values. The products were analysed and kinetic parameters determined for the cleavage of specific bonds of each substrate. Different affinities were found for a specific subsite depending on the pair of substrates used (results not shown) and the proportion of the formed products depended on substrate concentration and incubation time (data not shown). This effect of substrate concentration, especially apparent in hydrolysis of *p*-NPGlc$_2$ and *p*-NPGlc$_3$, motivated the choice of the method of Suganuma et al. [16]

(i) Catalytic efficiencies. — Nitrophenyl maltooligosaccharides were digested at initial concentration (S_0) less than 0.1 K_m and enzyme concentration (E_0) as indicated in Table 1. (S) at time t was determined as above. The plot of $\ln(S_0/S)$ vs. t is linear for PPA I and PPA II. The value of the slope gives k_{cat}/K_m (Table 1). For both isozymes, *p*-NPGlc$_2$ is a very poor substrate, the values increase sharply up to *p*-NPGlc$_4$ then reach a plateau value. All PPA I catalytic efficiencies were a little higher than those of PPA II, except for *p*-NPGlc$_3$ and *p*-NPGlc$_5$.

(ii) Cleavage frequencies. — The cleavage frequency ($p_i/\Sigma p_i$) indicates the binding mode of the corresponding substrate. For a given substrate, reproducible values were obtained at four incubation times; the mean value is given. The number of susceptible bonds and thus the subsite occupancy varies with the length of the substrate (Fig. 2).

Table 1
Catalytic efficiency of PPA I and PPA II determined at the indicated enzyme and *p*-nitrophenyl maltooligosaccharide concentration

Substrate	*p*-NPGlc$_2$	*p*-NPGlc$_3$	*p*-NPGlc$_4$	*p*-NPGlc$_5$	*p*-NPGlc$_6$	*p*-NPGlc$_7$
S_0 (μM)	40	40	40	40	40	40
E_0	34 μM	0.6 μM	5 nM	2.5 nM	2.5 nM	2.5 nM
k_{cat}/K_m ($mol^{-1}\ s^{-1}$)						
PPA I	15.6	3.33×10^3	1.16×10^6	4.18×10^6	5.10×10^6	5.78×10^6
PPA II	14.6	7.67×10^3	9.63×10^5	4.20×10^6	3.82×10^6	4.45×10^6

Two bonds are hydrolyzed in the *p*-NPGlc$_2$, the major cleavage leads to the liberation of *p*-nitrophenol, favouring binding mode 1 (bm 1). Also two bonds are cut in *p*-NPGlc$_3$ but the major cut leads to the liberation of *p*-NPGlc (bm 2). Two cleavages occur in the tetraoside, with a different frequency for PPA I while at about the same frequency for PPA II, yielding *p*-NPGlc$_2$ (bm 3) and *p*-NPGlc (bm 2), respectively. Remarkably, *p*-NPGlc$_5$ hydrolysis gives maltotriose and *p*-NPGlc$_2$, indicating binding mode 3. *p*-NPGlc$_6$ is cut almost equally to *p*-NPGlc$_2$ (bm 3) and *p*-NPGlc$_3$ (bm 4). Three internal bonds are hydrolysed in the heptaoside. PPA I gives in decreasing amount: *p*-NPGlc$_4$ (bm 5), *p*-NPGlc$_2$ (bm 3), and *p*-NPGlc$_3$ (bm 4). While PPA II produces *p*-NPGlc$_2$, *p*-NPGlc$_4$, and *p*-NPGlc$_3$.

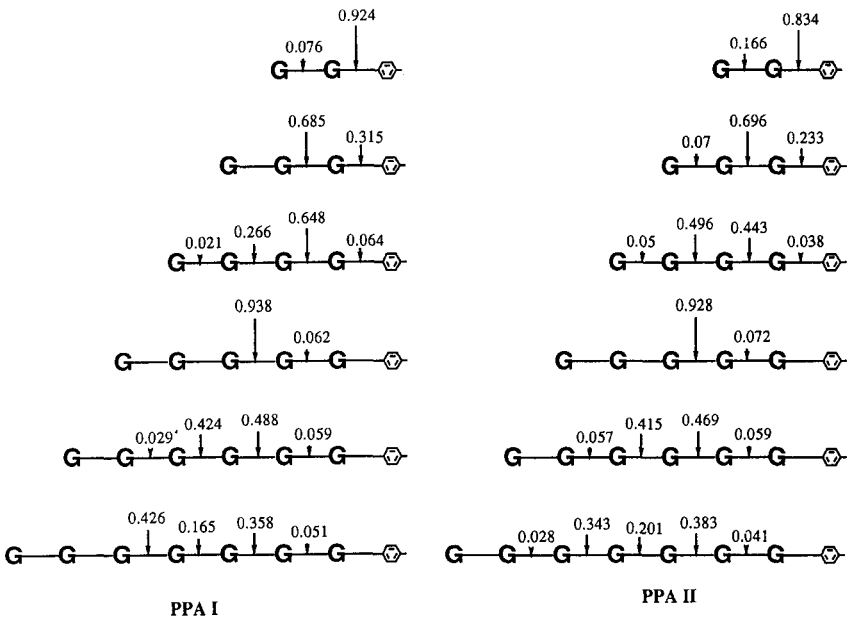

Fig. 2. Cleavage frequency of *p*-nitrophenyl maltooligosaccharides ($n = 2$–7) at low concentration ($< 0.1\ K_m$). The hydrolysis was catalyzed by PPA I (left) and PPA II (right). The concentration of enzymes and substrates are given in Table 1. Incubation volume: 100–200 μL. Incubation times are as in the Experimental section. The frequency is expressed as mol/mol.

(iii) Calculation of affinities (A_i) *of the glucose residue at the subsites of PPA I and PPA II.* — Only substrates covering the catalytic site were considered for A_i calculation. All subsite affinities, except A_{-1}, were obtained by subtracting the binding energies of a pair of substrates. Where possible several pairs of substrates were used. Binding energies were calculated using the kinetic data (Table 1) and the cleavage frequencies (Fig. 2). A_{-1} was calculated by taking into account the binding energy of the longest substrate (p-NPGlc$_7$) in a given binding mode and the affinities of the other subsites. The detailed calculation for PPA I is reported.

The affinity at subsite -6 was obtained by subtracting the binding energy of the p-NPGlc$_6$ (bm 2) from that of the p-NPGlc$_7$ in the same binding mode:

$$A_{-6} = B_{7,2} - B_{6,2} = -0.598 \text{ kJ/mol}$$

The affinity at subsite -5 is obtained from two different pairs of substrate:

$$A_{-5} = B_{7,3} - B_{6,3} = -0.196 \text{ kJ/mol}$$
$$= B_{6,2} - B_{5,2} = 0.000 \text{ kJ/mol}$$

The average value is -0.098 kJ/mol.

A_{-4} (kJ/mol) can be obtained using three pairs of substrate:

$$B_{7,4} - B_{6,4} = -1.509$$
$$B_{6,3} - B_{5,3} = -1.216$$
$$B_{5,2} - B_{4,2} = -1.346$$

The average is $A_{-4} = -1.359$ kJ/mol.

A_{-3} (kJ/mol) can be obtained in two ways:

$$B_{7,5} - B_{6,5} = 4.832$$
$$B_{5,3} - B_{4,3} = 4.941$$

The values are quite close. The average value is $A_{-3} = 4.886$ kJ/mol.

A_{-2} can be obtained only with short substrates ($n = 2,3,4$) and was not calculated as above, instead:

$$A_{-2} + A_{-3} = B_{6,4} - B_{4,4} = 9.05 \text{ kJ/mol}$$

then

$$A_{-2} = 9.05 - A_{-3} = 4.163 \text{ kJ/mol.}$$

A_1 (kJ/mol) can be calculated using one pair, assuming that the p-NP moiety has equivalent affinity for the subsites considered:

$$A_1 = B_{5,2} - B_{4,1} = 5.258 \text{ kJ/mol.}$$

A_2 (kJ/mol) can be calculated using three pairs:

$$B_{7,3} - B_{6,2} = 5.020$$
$$B_{6,3} - B_{5,2} = 5.354$$
$$B_{5,3} - B_{4,2} = 5.087$$

The average value is:

$$A_2 = 5.154 \text{ kJ/mol.}$$

For the calculation of A_3, two pairs can be used:

$$B_{7,4} - B_{6,3} = -1.818$$

$$B_{6,4} - B_{5,3} = -1.525$$

The average value is:

$$A_3 = -1.672 \text{ kJ/mol.}$$

In the same way one obtains:

$$A_4 = B_{7,5} - B_{6,4} = -0.163 \text{ kJ/mol}$$

and

$$A_5 = B_{7,6} - B_{6,5} = -1.476 \text{ kJ/mol}$$

The affinity of the catalytic subsite (A_{-1}), is calculated using the binding energy of p-NPGlc$_7$, for each of its binding modes. Binding mode 2 is given as an example:

$$B_{7,2} = RT \ln\left[(k_{cat}/K_m)_7 \cdot \left(p_i/\sum_1^5 p_i\right)/0.018k_{int}\right]$$

Where $p_i = (p\text{-NPGlc})$ and $\sum_1^5 p_i = (p\text{-NPGlc}) + (p\text{-NPGlc}_2) + (p\text{-NPGlc}_3) + (p\text{-NPGlc}_4) + (p\text{-NPGlc}_5)$. $k_{int} = 1820 \text{ s}^{-1}$ is the k_{cat} determined using amylose as a substrate. For PPA II, $k_{int} = 1700 \text{ s}^{-1}$.

$$B_{7,2} = \sum_{-6}^{1} A_i = A_{-6} + A_{-5} + A_{-4} + A_{-3} + A_{-2} + A_{-1} + A_1 = 22.363 \text{ kJ/mol}$$

then

$$A_{-1} = 10.11 \text{ kJ/mol}$$

From other binding modes (3,4,5 and 6), $A_{-1} = 9.982$, 9.932, 10.074, and 10.015 kJ/mol, respectively. The average value is: 10.03 kJ/mol.

The affinities hereabove calculated are summarized in Table 2. The energetic profile is similar for both amylases (Fig. 3). The active centre of PPA I and PPA II comprises only 5 subsites ($-3, -2, -1$, 1 and 2) with a positive value. Remarkably, the affinity of the catalytic subsite is the highest (10.03, 10.19 kJ/mol). Other values (A_{-6}, A_{-5}, A_{-4}, A_3, A_4 and A_5) are slightly negative excepting A_4 for PPA II and/or close to zero, and thus not meaningful.

The PPA II profile differs from the one of PPA I by having a lower affinity at subsite 1 and a higher affinity at subsite -3.

Table 2
Affinity (A_i) of the indicated subsite at the active centre of PPA I and PPA II. Values are expressed in kJ/mol

Isozyme	Subsite number										
	−6	−5	−4	−3	−2	−1	1	2	3	4	5
PPA I	−0.598	−0.1	−1.359	4.886	4.163	10.03	5.25	5.154	−1.672	−0.163	−1.476
PPA II	−0.017	−0.379	−2.024	7.009	4.021	10.191	3.626	4.836	−2.291	−0.397	

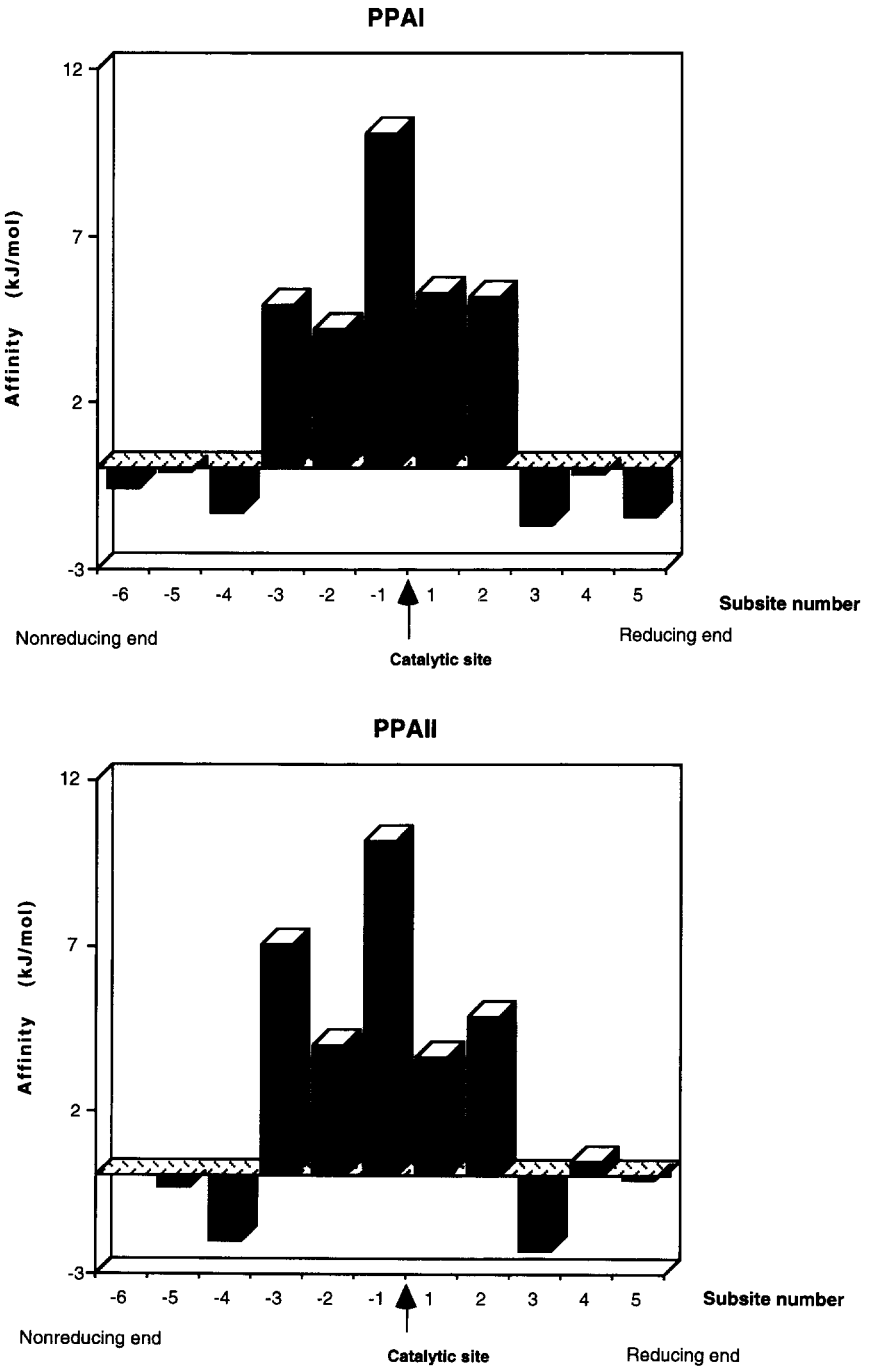

Fig. 3. Porcine pancreatic alpha-amylase I and II energetic profiles. Arrow indicates the catalytic site.

Finally, theoretical values of k_{cat}/K_m were calculated from the affinities obtained. An excellent agreement was found between theoretical and experimental values in the case of p-NPGlc$_4$, p-NPGlc$_5$, p-NPGlc$_6$, and p-NPGlc$_7$ while those calculated from shorter substrates differ by several orders of magnitude (results not shown).

4. Discussion

Subsite occupancy. — Analysis of products reveals which subsites of the active centre are occupied in a given binding mode. To identify the products with respect to the reducing/nonreducing end, some authors have used radioactive glucose to label the reducing end [1,25,26]; others, as we did, have used either nitrophenyl or phenyl maltooligosaccharides [27,28], the aglycone group being attached to the reducing glucose. The question then arises how the nitrophenyl group interacts at the active centre. In the present study, only the productive complexes have been considered.

In their work [1], Robyt and French have used a mixture of both amylase isozymes. More recently, Ishizuka et al. [26] reported cleavage distribution of maltooligosaccharides catalyzed by PPA II with results close to those of Robyt and French [1]. Comparison with our results gives information on the interaction of the p-nitrophenyl group with a given subsite. The cleavage frequencies of Glc$_3$ and p-NPGlc$_2$ are very close, the same pattern was observed for Glc$_4$ and p-NPGlc$_3$. For short substrates, the p-NP moiety would thus be equivalent to a glucosyl residue as suggested by MacGregor et al. [29]. This is not true with longer substrates, Glc$_5$ (1 binding mode) occupies the active centre of PPA in a different way as compared to p-NPGlc$_4$ (4 binding modes) while Glc$_5$ and p-NPGlc$_5$ are split similarly, suggesting that the p-NP moiety only weakly interacts with the corresponding subsite. The bond cleavage of Glc$_6$ and Glc$_7$ is different from the respective nitrophenylated derivatives, but still the major cleavage, and thus the most favoured binding mode, is no. 2 for Glc$_6$ and Glc$_7$ and no. 3 for p-NPGlc$_6$ and p-NPGlc$_7$, indicating that the nitrophenyl group has only little influence on the cleavage pattern.

Subsite affinities. — A_i determined from pairs of substrates with $n \geqslant 4$ differ from values calculated from shorter length substrates (not shown). Similar difference has been observed in barley alpha-amylase [27]. This might result from either transglycosylation or different k_{int} values or subsite interdependence or bimolecular binding [30] which occurs with small substrates.

Our results cannot be compared precisely to the ones of Seigner et al. [15] since these authors have used kinetic parameters determined from hydrolysis of short substrates ($n = 2$–4). In the present work, considering the subsites located at the nonreducing-end side (-1 to -6), the affinity of the p-NP moiety is eliminated in the subtraction and does not interfere with the calculation; while, in the calculation of the affinity of the subsites at the reducing-end side (1, 2, 3 ...), pairs of substrates with different binding modes have been used. We need not know the binding affinity of the p-NP moiety, but postulate that its affinity is equivalent for the subsites considered. This seems a reasonable hypothesis since the values obtained from various pairs of substrates are close. Also very close A_{-1} values were obtained regardless of the binding mode of p-NPGlc$_7$, in spite of the low accuracy for its calculation as compared to other subsites.

The binding energy of eleven glucosyl residues were calculated. Our results, with five positive affinity subsites, agree with Robyt and French proposal [1]. Obviously, affinities with slightly negative values are meaningless, but negative subsite affinities have been found by Thoma et al. [34] in *B. amyloliquefaciens* alpha-amylase. In this work, their affinity was adjusted to zero. In the present study, they may indicate that some of the assumptions made (rapid equilibrium, no subsite interdependence, and k_{int} constant) are only approximate.

The PPA I and PPA II energetic profiles differ with respect to the subsites -3 and 1. Experimental error may explain A_1 since it was calculated from a single pair of substrates in a binding mode, leading to a low cleavage frequency. The calculation of A_{-3} relies on 2 pairs of substrates which give the same result, thus confirming the difference between PPA I and PPA II. The catalytic efficiency of PPA I and PPA II increases with chain length, reaching a plateau for $n = 5$. This demonstrates that maximum amylolytic activity requires occupancy of all subsites. The energetic profiles of several alpha-amylases from bacteria, fungi, yeast, and plants have been determined. Alpha-amylases can be classified into three groups: barley with 9–10 subsites (-6, 4) [27] or (-6, 3) [32] the *Aspergillus oryzae* containing 9 subsites (-4, $+5$) [16,33] and the mammalian/*Bacillus subtilis* saccharifying amylases with 5 subsites (-3, 2) [1,28]. All alpha-amylases studied with the exception of the porcine enzyme, contain a central catalytic subsite with a negative affinity. In contrast, the energetic profiles of PPA I and PPA II show a high positive affinity at this subsite. It would be of interest to establish if this property is specific to mammalian alpha-amylases particular structural organization of the active site. X-ray structure analysis of PPA I-acarbose (a carbohydrate inhibitor) complex shows detailed interactions in all five subsites, with the acarviosine unit present in subsite -1 and 1, the three other subsites interacting with a glucosyl residue [34]. The active centre region is a V-shaped cavity, the catalytic subsite (-1) is at the most internal position at 6 Å from the chloride ion, an activator specific for mammalian amylases [35]. Subsites -2, 1, and 2 are located at the surface edge of the cavity, subsite -1 is deeper, while subsite -3 is more exposed to the solvent. The location of the catalytic subsite is very likely related to its high binding affinity.

Abbreviations: *p*-NP, *p*-NPGlc, *p*-NPGlc$_2$, *p*-NPGlc$_3$, *p*-NPGlc$_4$, *p*-NPGlc$_5$, *p*-NPGlc$_6$ and *p*-NPGlc$_7$ were used, respectively, for 4-nitrophenol, 4-nitrophenyl-α-D-glucopyranoside, 4-nitrophenyl-α-maltoside, 4-nitrophenyl-α-maltotrioside, 4-nitrophenyl-α-maltotetraoside, 4-nitrophenyl-α-maltopentaoside, 4-nitrophenyl-α-maltohexaoside, and 4-nitrophenyl-α-maltoheptaoside.

Acknowledgements

We are very much indebted to Dr A.W. and A.E. MacGregor for very helpful advice in the preparation of this manuscript.

We are very grateful to Dr V. Desseaux for performing the electrofocusing analysis of PPA I and PPA II.

References

[1] J.F. Robyt and D. French, *J. Biol. Chem.*, 245 (1970) 3917–3927.
[2] G. Marchis Mouren and V. Desseaux, *Biochem. Life Sci. Adv.*, 8 (1989) 91–96.
[3] G. Marchis Mouren and L. Pasero, *Biochim. Biophys. Acta*, 140 (1967) 366–368.
[4] G. Buisson, E. Duee, R. Haser, and F. Payan, *EMBO J.*, 6 (1987) 3909–3916.
[5] M. Qian, R. Haser and F. Payan, *J. Mol. Biol.*, 231 (1993) 785–799.
[6] S.B. Larson, A. Greenwood, D. Caseio, J. Day, and A. MacPherson, *J. Mol. Biol.*, 235 (1994) 1560–1584.
[7] Y. Matsuura, M. Kusunoki, W. Harada, and M. Kakudo, *J. Biochem.*, 95 (1984) 697–702.
[8] E. Boel, L. Brady, A. Brzozowski, Z. Derewenda, G. Dodson, V. Jensen, S. Petersen, H. Swift, L. Thim, and H.F. Woldike, *Biochemistry*, 29 (1990) 6244–6249.
[9] A. Kadziola, J. Abe, B. Svensson, and R. Haser, *J. Mol. Biol.*, 239 (1994) 104–121.
[10] E.A. MacGregor, *J. Protein Chem.*, 7 (1988) 399–415.
[11] E. Raimbaud, A. Buléon, S. Pérez, and B. Henrissat, *Int. J. Biol. Macromol.*, 11 (1989) 217–225.
[12] G.K. Farber and G.A. Petsko, *TIBS*, 15 (1990) 228–234.
[13] F. Payan, R. Haser, M. Pierrot, M. Frey, J.P. Astier, B. Abadie, E. Duee, and G. Buisson, *Acta Crystallogr., Sect. B*, 36 (1980) 416–421.
[14] G. Buisson, F. Duee, F. Payan, and R. Haser, *Food Hydrocolloids*, 1 (1987) 399–406.
[15] C. Seigner, E. Prodanov, and G. Marchis Mouren, *Biochim. Biophys. Acta.*, 913 (1987) 200–209.
[16] Y. Suganuma, R. Masuno, M. Ohnishi and K. Hiromi, *J. Biochem.*, 84 (1978) 293–316.
[17] M. Granger, B. Abadie, Y. Mazzei, and G. Marchis Mouren, *FEBS Lett.*, 50 (1975) 276–278.
[18] S. Dygert, L.H. Li, and J. Thoma, *Anal. Biochem.*, 13 (1965) 367–374.
[19] K. Hiromi, *Biochem. Biophys. Res. Commun.*, 40 (1970) 1–6.
[20] L. Paséro, Y. Pierron, B. Abadie, Y. Chicheportiche, and G. Marchis Mouren, *Biochim. Biophys. Acta*, 869 (1986) 147–157.
[21] I. Kluh, *FEBS Lett.*, 136 (1981) 231–234.
[22] B. Meloun, I. Kluh, and L. Moravek, *Collect. Czech. Chem. Commun.*, 45 (1980) 2572–2582.
[23] F. Payan, personal communication.
[24] J. Thoma, G. Rao, C. Brothers, and J. Spradlin, *J. Biol. Chem.*, 246 (1971) 5621–5635.
[25] I. Matsui, K. Ishikawa, E. Matsui, S. Miyairi, S. Fukui, and K. Honda, *J. Biochem.*, 109 (1991) 566–569.
[26] Y. Ishizuka, Y. Sakano, and T. Kobayashi, *Agric. Biol. Chem.*, 50 (1986) 3019–3023.
[27] E.H. Ajandouz, J. Abe, B. Svensson, and G. Marchis Mouren, *Biochim. Biophys. Acta*, 1159 (1992) 193–202.
[28] Y. Nagamine, K. Omichi, and T. Ikenaka, *J. Biochem.*, 104 (1988) 409–415.
[29] A.W. MacGregor, J.E. Morgan, and E.A. MacGregor, *Carbohydr. Res.*, 227 (1992) 301–313.
[30] C. Seigner, E. Prodanov, and G. Marchis Mouren, *Eur. J. Biochem.*, 148 (1985) 161–168.
[31] J.A. Thoma, C. Brothers, and J. Spradlin, *Biochemistry*, 9 (1970) 1768–1774.
[32] E.A. MacGregor and A.W. MacGregor, *Carbohydr. Res.*, 142 (1985) 223–236.
[33] K. Hiromi, M. Ohnishi, and A. Tanaki, *Mol. Cell. Biochem.*, 51 (1983) 79–85.
[34] M. Qian, R. Haser, G. Buisson, E. Duee, and F. Payan, *Biochemistry*, 33 (1994) 6284–6294.
[35] A. Levitzki and M. Steer, *Eur. J. Biochem.*, 41 (1974) 171–180.